DETECTION AND TRACKING OF VORTICES AND SADDLE POINTS FROM SST DATA*

Qing Yang and Bahram Parvin
Information and Computing Sciences Division
Lawrence Berkeley National Laboratory
Berkeley, CA 94720
www-itg.lbl.gov/VISION

Abstract

We extend the Horn-Schunck model of flow field computation to incorporate incompressibility for tracking fluid motion. This is expressed as a zero-divergence constraint in the variational problem and implemented with a mutigrid approach for efficient computation. Additionally, we show effective detection and tracking of singular events, such as vortices and saddle points, from the velocity field. We have applied our approach to 12 years of AVHRR data at 18 Km resolution and tabulated a feature database for data mining. Our analysis indicates preferred localization of singular events over long time scales.

1 Introduction

Current environmental satellites provide oceanographic images with different types of physical measurements. In this paper, we focus on sea surface temperature (SST) data. These data are collected using AVHRR satellite sensors, then downlinked to the University of Miami for automatic calibration and computation of geophysical fields by combining the satellite swath data. It is highly desirable to represent a massive amount of SST data for abstraction and subsequent data mining. One possible abstraction relies on localization of vortices and saddle points from feature velocities. Ocean vortices are an important component of global circulation because they are an efficient transport and mixing mechanism for salt/freshwater, heat, plankton communities, and nutrients. Saddle points are nonlinear points that are essentially chaotic events. We will show that these points exist in the ocean and that they can be detected and tracked from SST data. Furthermore, from an informatic point of view, an abstraction based on vortices and saddle points provides a compact representation of underlying feature velocities. Our method is efficient, robust, and has been tested on real data. Such a feature-based representation provides the enabling framework for subsequent climate trend analysis, the study of ocean variability, and data mining. Moreover, such an abstraction provides the basis for comparative studies between simulation and observational data. Detection of vortices and saddle points relies on computing feature velocity. Here, we introduce a novel formulation of flow field computation that incorporates an incompressibility constraint for tracking fluid motion. The proposed technique is then implemented through a multigrid representation to reduce the computational complexity.

In Section 2, we review previous work in flow field computation. Section 3 provides the details of our approach, including flow computation, feature detection, statistical analysis using feature database, and experimental results on real data. Section 4 concludes the paper.

2 Previous Work

Measurement and analysis of feature velocities is often referred to computation of optical flow in the imaging literature. Review and enhancement of these techniques can be found in [3, 7]. Recent efforts have focused on defining a set of basis functions for recovery of smooth motion [4]. In this approach, the motion field discontinuity is expressed as a linear combination of a small number of the basis motions. The emphasis is toward a parameterized model of motion for explanation and estimation. The approach is noniterative and thus adequate for real-time processing. Cohen and Herlin [5] proposed a nonquadratic regularization technique for solving the optical flow constraint equation and applied it to oceanographic images. The approach is applicable to irregularly spaced images with missing data. The regularization problem was solved by finite difference method with finer tessellation near the motion boundary. Amini [1] extended Schunck's equation

*This work is supported by the Director, Office of Energy Science Research, Office of Computation and Technology Research, Mathematical, Information, and Computational Sciences Division of the U. S. Department of Energy under Contract No. DE-AC03-76SF00098 with the University of California. The LBNL publication number is 44269.
E-mail: qyang,parvin@george.lbl.gov

to include fluid X-ray images of contrast velocity in arteries. This was expressed in terms of zero divergence of flow field to *simplify* the solution. His method applies to X-ray images, but it cannot be used to compute motion in SST images due to its computational complexity. Another drawback of his approach is that the corresponding partial differential equation is of a higher order. Oceanic satellite images (or those generated from high resolution simulation models) have unique physical constraints in terms of fluid incompressibility. Additionally, because the data resides in the spherical coordinate system, it requires special treatment. Our formulation does not require solution of higher order PDEs, and it has been implemented in a multigrid framework for better computational efficiency. Feature extraction from flow field measurements often relies on eigenvalue analysis from the local Jacobian. We will present an elegant approach for detection of vortices and saddle points that has proved to work effectively in our data sets.

3 Approach

In this section, we will describe a set of algorithms to compute feature velocities from consecutive images of sea surface temperature data and to localize singular events (saddle points and vortices) from velocity vectors.

3.1 Computation of feature velocities

Let $I(x, y, t)$ be the image at time t, with (u, v) as the velocity vector at each point. The flow field equation with brightness constancy assumption is given by:

$$\frac{dI(x,y,t)}{dt} = I_x u + I_y v + I_t = 0 \qquad (1)$$

where the subscripts x, y, and t represent the partial derivatives. Horn and Schunck [6] constrained the problem by incorporating local smoothness in the flow. This is given by:

$$\begin{aligned}(u^*, v^*) \quad &= \arg\min E := \int\int (I_x u + I_y v + I_t)^2 \\ &\quad +\alpha(|\nabla u|^2 + |\nabla v|^2) dx dy\end{aligned}$$

where α is the weighting factor of the smoothness term. Note that spherical coordinates should be used in this equation. We will discuss the problem of coordinate transformation later. The velocity vector due to (incompressible) fluid motion has to have zero divergence at each point: $u_x + v_y = -w_z$ Since w is difficult to estimate, the above constraint is applied in a weak sense, e.g., $u_x + v_y = 0$. In this context, incompressibility is enforced along the temperature-gradient (normal to iso-thermals). A vector field with zero-divergence does not contain sinks and sources.

This constraint is expressed as a penalty term in the energy functional:

$$\begin{aligned}(u^*_\beta, v^*_\beta) \quad &= arg\min E := \tfrac{1}{2}\int\int [(I_x u + I_y v + I_t)^2 \\ &\quad +\alpha(|\nabla u|^2 + |\nabla v|^2) + \beta(u_x + v_y)^2] dx dy\end{aligned}$$

The Euler-Lagrange equation of this equation is
$-I_x(I_x u + I_y v + I_t) + (\alpha+\beta)u_{xx} + \alpha u_{yy} + \beta v_{xy} = 0$
$-I_y(I_x u + I_y v + I_t) + \alpha v_{xx} + (\alpha+\beta)v_{yy} + \beta u_{xy} = 0$
which can be solved using finite difference approximation. The algorithm is iterative and converges to a local minimum solution, satisfying smoothness and zero-divergence constraint.

The solution to the above equations is achieved through multigrid technique to reduce the computational complexity. Let h be the window size where finite differences are computed. Then by setting $h = 2^K, 2^{K-1}, \cdots, 1$ successively, we can propagate from coarse to fine grid through simple linear interpolation and refinement.

3.2 Evaluation of feature velocities

Both α and β of the regularization parameters are important for accurate measurement of feature velocities. There is a big difference between S^2 and R^2 in that their topological structures are not homomorphic. With respect to the quality of our measurements, we have compared our results to prior literature (Nov. 5, 1986 to Nov 18, 1997, Aoki et al. [2]) that indicates a motion field of 3-5cm/sec to the west from 35 to 40 N in the region 30 to 40°N and 140° E to 170° W. Our results for the same years indicate similar feature velocity in those regions, thus validating our measurements.

3.3 Detection of vortices and saddle points

Singularities in the flow field can provide a compact abstraction in the velocity field. This issue has been addressed in literature [8], where an algorithm based on the analysis of local Jacobian was proposed. Their approach is complex due to the fact that the flow field is not regularized. Here, we propose an alternative method for robust estimation of event detection and subsequent tracking of singularities.

Let $F = (u, v)$ be a vector field and J be a Jordan curve with no critical point on it. The index of J is defined by

$$\text{Index}(J) = \frac{1}{2\pi}\oint_J \frac{udv - vdu}{u^2 + v^2}$$

At each point P, we choose a small circle J_P around P and compute Index(J_P). The flow field (u, v) can then be classified according to:

1. The index of a vortex is equal to +1 (the classification of singular points in a vector field is given in [8]), and

2. The index of a saddle point is equal to -1.

There is no node in the vector field because of the zero-divergence constraint, but singularities do occur. Recall that a point (x, y) is singular iff $u(x, y) = 0$ and $v(x, y) = 0$. However, using this condition to localize singularities leads to computational instability. A better approach is to exploit the inherent local minimum velocity volume to simplify the problem. Thus,

- Step 1: Find all local minima of the velocity field, i.e., $\sqrt{u(x,y)^2 + v(x,y)^2}$
- Step 2: $\forall (x, y) \in S$:

  (1) Let $R = \frac{1}{2}\max\{r | S \bigcap J^r_{(x,y)} = \phi\}$ where $J^r_{(x,y)}$ is the circle centered at (x, y) with radius r.
  (2) Compute the index of $J^R_{(x,y)}$, that is,

$$\text{Index}(J^R_{(x,y)}) = \frac{1}{2\pi} \oint_{J^R_{(x,y)}} \frac{udv - vdu}{u^2 + v^2}$$

  (3) If $\text{Index}(J^R_{(x,y)}) = 0$, then (x, y) is not singular; if $\text{Index}(J^R_{(x,y)}) = 1$, then (x, y) is a vortex; if $\text{Index}(J^R_{(x,y)}) = -1$, then (x, y) is a saddle point.

One important characteristic of vortex is its "size." Here, we propose a simple definition. If a point a (x, y) is a vortex, then its size $R^*(x, y)$ can be defined as:

$$R^*(x, y) = \max\{R | \text{Index}(J^R_{(x,y)}) = 1\}$$

that is to say, $R^*(x, y)$ is the largest R such that the index of $J^R_{(x,y)}$ remains 1. Fig. 1 shows the feature velocities (date: the 200th day of the year 1992) corresponding to a pair of SST data. See the captions for more detail.

3.4 Analysis

We have processed SST data, at 18 Km resolution, from 1986 to 1998 to create a database for trend analysis and data mining. Each singular event is represented with a number of attributes that include year, season, date, spatial location, size, event type, temperature, wind vector, and precipitation. We have constructed seasonal and interannual probability density functions that rate the occurrences of vortices and saddle points. Table 1 shows the number of events in each season and year from 1986 to 1998.

Figure 2 shows preferred occurrences of events for a 12-year period (2190 images). The results clearly indicate preferred occurrences of events along the equator, Gulf Stream and to the north of it, and 40° S. These areas are the East Pacific instability region, the Gulf Stream vortices, the meander region, and the subpolar front of the Southern Oceans.

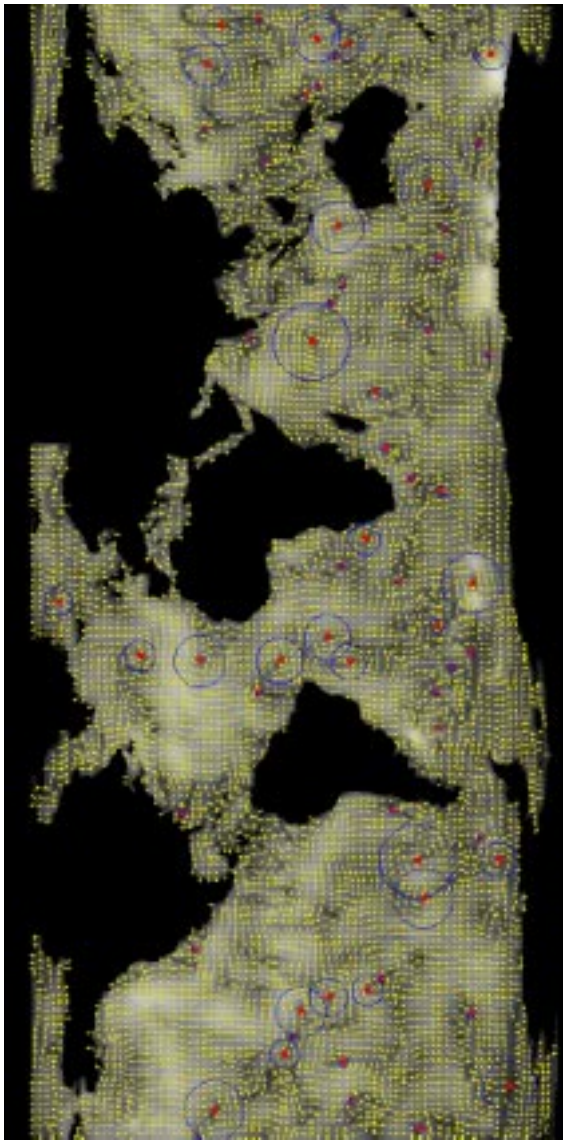

Figure 1: Feature velocities and computed vortices from SST: Feature directions are shown with arrows, and their corresponding magnitudes are shown with the underlying brightness map. Vortices are surrounded with a blue circle. This result is generated from a pair of consecutive images around day 200 from 1992.

Year	*Winter*	*Spring*	*Summer*	*Fall*
1986	5194	3991	5126	4425
1987	4970	3881	5382	4455
1988	5119	3991	5241	4854
1989	5051	4303	5060	4230
1990	4933	4183	5298	4470
1991	5166	4133	5542	4870
1992	5254	4273	5446	4617
1993	4988	4043	5247	4171
1994	5057	3942	5071	3380
1995	5109	4212	5089	4419
1996	5283	4090	5210	4847
1997	5422	4280	5278	4519
1998	5095	4074	5133	4534

Table 1: Number of events (vortices and saddle points) in each season and each year of SST data. Each event is represented with its date, location, size, and temperature in the database. It is also cross referenced with other fields for precipitation and wind stress measurements.

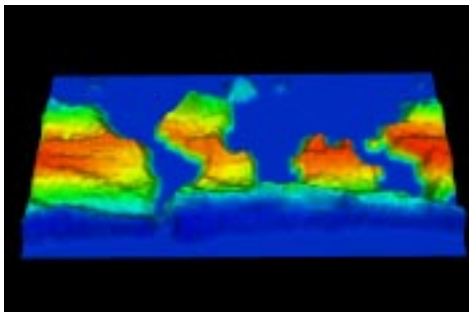

(a)

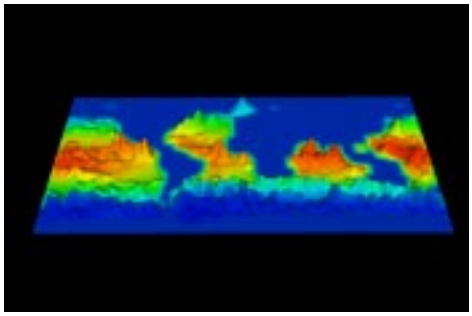

(b)

Figure 2: Frequency of occurrence of vortices and saddle points, shown at 1° resolution, from 1986 to 1998: (a) One view of all events; (b) PDF corresponding to the local maxima of each year accumulated over the 12 year period.

4 Conclusions

In this paper, we formulated motion computation in oceanographic images as a constrained variational problem with incompressibility constraint, which is generalization of Horn-Schunck's original work. A robust technique for detection of singularities (vortices and saddle points) in the velocity field was proposed, implemented, and shown on real data. The techniques were applied to 12 years of SST data. We have shown that singular events have a prefered localization and frequency of occurrence throughout the data. These include 40° S, Gulf Stream, and instability regions in the pacific.

Acknowledgement: The authors deeply appreciate valuable discussion and data supplied to us by Prof. Arthur Mariano of RSMAS at the University of Miami.

References

[1] A.A. Amini. A scalar function formulation for optical flow: Application to x-ray imaging. In *IEEE Workshop on BioMedical Imaging*, pages A:117–124, 1994.

[2] S. Aoki, S. Imawaki, and K. Ichikawa. Baroclinic disturbances propagating westward in the kuroshio extension region as seen by a satellite altimeter and radiometers. *Geophysical Research-Oceans*, 100:839–855, 1995.

[3] J.L. Barron, D.J. Fleet, and S.S. Beauchemin. Performance of optical flow techniques. In *CVPR92*, pages 236–242, 1992.

[4] M.J. Black and P. Anandan. The robust estimation of multiple motions: Parametric and piecewise-smooth flow-fields. *CVIU*, 63:75–104, 1996.

[5] I. Cohen and I. Herlin. A motion computation and interpretation framework for oceanographic satellite images. In *SCV95*, pages 13–18, 1995.

[6] B. K. P. Horn and B. G. Schunck. Determining optical flow. *Artificial Intelligence*, 17:185–203, 1981.

[7] S.H. Lai and B.C. Vemuri. Robust and efficient algorithms for optical flow computation. In *SCV95*, pages 455–460, 1995.

[8] A. R. Rao and R. C. Jain. Computerized flow field analysis: Oriented texture fields. *IEEE Transactions on Pattern Analysis and Machine Intelligence*, pages 225–270, 1994.